DOI: 10.1002/ejic.200800269

Lanthanide-Based Conjugates as Polyvalent Probes for Biological Labeling

Stéphanie Claudel-Gillet,[a] Jérôme Steibel,[b] Nicolas Weibel,[a] Thomas Chauvin,[c] Marc Port,[d] Isabelle Raynal,[d] Eva Toth,*[c] Raymond F. Ziessel,*[a] and Loïc J. Charbonnière*[a]

Keywords: Lanthanides / Bio-conjugation / Luminescence / Relaxivity / Time-resolved luminescence microscopy

A series of lanthanide complexes of [Ln**L**(H_2O)] composition, suitable for biological labeling has been studied, in which **L** is a strongly chelating ligand containing chromophoric bipyridylcarboxylate units and Ln = Sm, Eu, Gd, Tb, and Dy. For the Gd complex, a combined ^{17}O NMR and ^{1}H NMRD study has been performed. The water exchange rate obtained, $k_{ex}^{298} = (5.2 \pm 0.6) \times 10^6\ s^{-1}$, is slightly higher than those for $[Gd(dota)(H_2O)]^-$ or $[Gd(dtpa)(H_2O)]^{2-}$. Transformation of the uncoordinated carboxylate function of the ligand into an activated ester ensures covalent linking of the complex to bovine serum albumine (BSA). The relaxivity properties of the Gd complex labeled on BSA revealed a limited increase of both longitudinal and transversal relaxivities. This can be related to the partial replacement of the inner-sphere water molecules by coordinating functions of the protein. Additionally, the Sm and Dy complexes are described and chemically characterized. Their photophysical properties were investigated by means of absorption, steady-state and time-resolved spectroscopy, evidencing efficient photosensitization of the lanthanide emission by ligand excitation (antenna effect). Luminescence lifetime measurements confirmed the presence of a water molecule in the first coordination sphere that partly explained the relatively poor luminescence properties of the Dy and Sm complexes in aqueous solutions. The spectroscopic properties of the series of complexes are questioned in terms of time-resolved acquisition techniques. Finally, their availability for use in time-resolved luminescence microscopy is demonstrated by staining experiments of rat brain slices, where the complex showed enhanced localization in some hydrophilic regions of the blood–brain barrier (BBB).

Introduction

Applications of lanthanide complexes in biological analysis have been mainly focused on two distinct fields of research, dealing with: (1) the use of paramagnetic complexes as contrast agents for magnetic resonance imaging (MRI)[1] or as shift agents for protein NMR[2] and (2) as luminescent complexes for labeling experiments in time-resolved fluoroimmunoassays,[3] luminescent resonant energy transfer,[4] and time-resolved luminescence microscopy (TRLM).[5] As a result of their lack of stereoelectronic preferences and their very similar ionic radii [$\Delta R < 5\%$, from Sm to Dy for a coordination number (CN) of 9],[6] Sm to Dy complexes are often isostructural. As a matter of fact, the different applications usually require different ligand designs. On the one hand, to ensure a high efficacy for MRI applications, Gd-based relaxation agents require at least one vacant coordination site in order to have a water molecule in the "inner sphere" of the lanthanide cation. On the other hand, for the luminescent labels one would prefer the water molecules to be as far away as possible from the lanthanide atom to avoid detrimental nonradiative deactivation pathways associated with the presence of OH oscillators.[7] The use of a ubiquitous ligand for the preparation of lanthanide complexes showing both relaxivity and luminescence properties then appears conflicting. Nevertheless, while restricting the mechanism of relaxation of Gd complexes to second- or outer-sphere interactions is revealed as detrimental to achieving high relaxivity, the presence of first-sphere-coordinated water molecules in luminescent lanthanide complexes can in some cases be accommodated with interesting photophysical properties.[8]

A plethora of complexes, dealing either with the relaxometric or with the photophysical properties have been studied, but scarcely with a combination of both. The main explanation probably stems from the absence of chromophoric units on most of the Gd complexes, which are essential for luminescent lanthanide chelates. The chromophoric units allow for an efficient collection of photons that generate Ln-centered excited states, through the so-called an-

[a] Laboratoire de Chimie Moléculaire, UMR 7509, ECPM, 25 rue Becquerel, 67087 Strasbourg Cedex 02, France
Fax: +33-3-90-24-2689
E-mail: charbonn@chimie.u-strasbg.fr
[b] Laboratoire d'Imagerie et de Neurosciences Cognitives, Faculté de Médecine, 4 rue Kirschleger, 67085 Strasbourg Cedex, France
[c] Centre de Biophysique Moléculaire, CNRS, Rue Charles-Sadron, 45071 Orleans Cedex 2, France
[d] Guerbet, B. P. 57400, 95943 Roissy Charles de Gaulle Cedex, France
Supporting information for this article is available on the WWW under http://www.eurjic.org or from the author.

tenna effect.[9] Introduction of chromophoric arms on dota-like derivatives[10,11] or of pyridyl-[12] and polypyridyl-based[13] macrocyclic structures paved the way, but the goal of a polyvalent family of lanthanide labels covalently grafted on biomolecules has remained unachievable up to now.

We have recently reported on the excellent photophysical properties of Tb and Eu complexes with ligand **L** (Scheme 1),[14] that can easily be tethered to amino residues of proteins with retention of their photophysical properties by means of the activation of an uncoordinated carboxylate moiety such as in **L***. In this contribution, the scope of the study of lanthanide complexes of **L** is extended to the photophysical characterization of Sm and Dy complexes together with a ^{1}H and ^{17}O relaxation study of the Gd analogue. The application of luminescent or relaxivity enhancement properties are applied to biological systems by staining experiments with luminescence microscopy observations and labeling experiments of a protein with Gd to study the impact on the relaxivity.

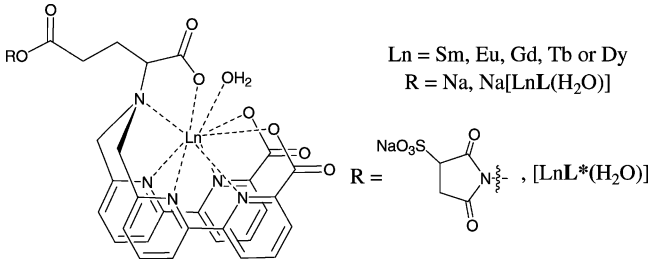

Scheme 1.

Results and Discussion

Relaxivity Properties of Na[GdL(H$_2$O)]

The efficiency of a Gd^{3+} complex as a contrast agent in MRI is commonly expressed by its relaxivity. Relaxivity, r_1, is defined as the paramagnetic enhancement of the longitudinal water proton relaxation rate in the presence of a 1 mM concentration of Gd^{3+}. The relaxivity is directly related to the microscopic properties of the complex, the most important being water exchange, rotational dynamics, and electron-spin relaxation. The successful use of Gd^{3+}-based contrast agents in clinical diagnostics prompted important research efforts to further optimize the efficiency of the complexes, by a rational optimization of the parameters that affect relaxivity. In particular, a large body of data has been accumulated on the water exchange properties of Gd^{3+} complexes.[1] Nevertheless, the majority of these data is restricted to the classical families of dota or dtpa derivatives, and relatively little is known on Gd^{3+} complexes of structurally very different chelators such as polyheterocyclic-based structures as in **L**. Evidently, the limited solubility of the Na[Ln**L**(H$_2$O)] complexes prevents any contrast agent application in MRI; however, it seemed interesting to gain insight into the water-exchange characteristics on the Gd^{3+} complex of this bis(bipyridine)-based ligand.

We have performed variable-temperature ^{17}O transverse relaxation rate measurements at 11.7 T in an aqueous solution of [Gd**L**(H$_2$O)]$^-$ to directly assess the rate of water exchange. In addition, the proton relaxivities have been measured at 310 K in the proton Larmor frequency range of 0.01–300 MHz (^{1}H NMRD profile), and the results are presented in Figure 1. The ^{17}O NMR and the ^{1}H relaxation rate data were analyzed simultaneously according to the common Solomon–Bloembergen–Morgan theory[15] that relates the observed paramagnetic relaxation rates to the microscopic parameters of the complex (see Supporting Information for full mathematical treatment of the fitting). The curve of the ^{17}O transverse relaxation rates vs. temperature shows that the system is in the slow exchange regime at low temperatures (below ca. 310 K) and in the fast exchange regime at higher temperatures. In the slow exchange regime, the relaxation rates are directly determined by the water exchange rate, which implies that the exchange rate can be obtained with a good certitude.

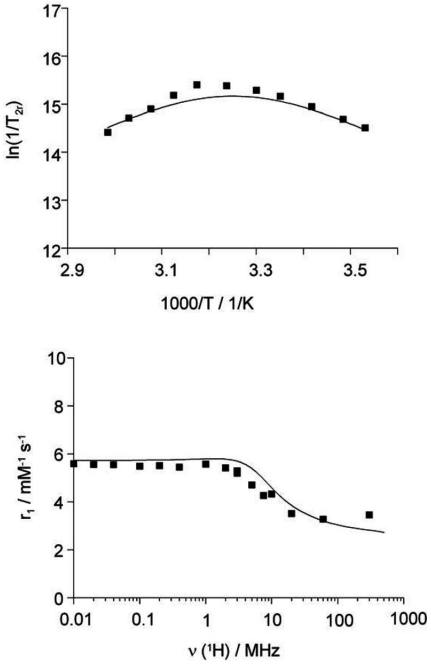

Figure 1. Variable temperature, reduced transverse ^{17}O relaxation rates at 11.7 T (top) and field-dependent ^{1}H relaxivities (NMRD profile) at 37 °C measured for Gd**L**(H$_2$O)$^-$. The curves represent the simultaneous fit of all experimental data to the Solomon–Bloembergen–Morgan theory (see text).

The hydration number was fixed to q = 1 as determined by luminescence for the Eu^{3+} and Tb analogues,[14] flanking Gd in the 4f series. In the simultaneous fit, the rate, the activation enthalpy and entropy of the water exchange, k_{ex}^{298}, $\Delta H^{\ddagger}$ and $\Delta S^{\ddagger}$, respectively, as well as the scalar coupling constant, $A/\hbar$, are determined by the ^{17}O transverse relaxation rates. The rotational correlation time, τ_R^{310}, is obtained from the proton relaxivity data, whereas the electron spin relaxation parameters, such as the correlation time for the modulation of the zero-field splitting, τ_v^{298}, and the mean zero field splitting energy, Δ^2, are related to both ^{17}O

and ^1H relaxation rates. Some of the parameters have been fixed to common values: the distance of Gd^{3+} from the water proton (r_{GdH}) was fixed to 3.1 Å; the distance of the closest approach of the outer sphere water molecules to Gd^{3+} (a) was fixed to 3.6 Å. The activation energy for τ_v, E_V had to be fixed to 1 kJ mol^{-1}, otherwise the fit converged to negative values. For the scalar coupling constant we used $A/\hbar = -3.8 \times 10^6$ rad s^{-1}, a typical value for monohydrated Gd^{3+} complexes.[16] The diffusion constant of the complex, which enters in the description of the outer-sphere contribution to relaxivity, was fixed to $D_{GdH}^{310} = 3.7 \times 10^{-9}$ m^2 s^{-1}. The fit is depicted in Figure 1, and the parameters obtained are listed and compared to those of the most common contrast agents $[Gd(dtpa)(H_2O)]^{2-}$ and $[Gd(dota)(H_2O)]^-$ in Table 1. The equations used in the fit are given in the Supporting Information.

Table 1. Fitted parameters for the $[Gd\mathbf{L}(H_2O)]^-$ complex in water and comparison with the monoaqua complexes $[Gd(dtpa)(H_2O)]^{2-}$ and $[Gd(dota)(H_2O)]^-$.[16]

	$[Gd(dtpa)(H_2O)]^{2-}$[a]	$[Gd(dota)(H_2O)]^-$[a]	$[Gd\mathbf{L}(H_2O)]^-$
k_{ex}^{298} [10^6 s^{-1}]	3.3	4.1	5.2 ± 0.6
$\Delta H^{\ddagger}$ [kJ mol^{-1}]	51.6	49.8	39 ± 3
$\Delta S^{\ddagger}$ [J mol^{-1} K^{-1}]	+53	+49	+21 ± 8
τ_R^{310} [10^{-12} s]	32	42	53 ± 11
τ_v^{298} [10^{-12} s]	25	11	25 ± 8
Δ^2 [10^{20} s^{-2}]	0.46	0.16	0.5 ± 0.1

[a] Ref.[16]

The water exchange rate on $[Gd\mathbf{L}(H_2O)]^-$ is only slightly higher than those on $[Gd(dtpa)(H_2O)]^{2-}$ or $[Gd(dota)(H_2O)]^-$, and the activation entropy $\Delta S^{\ddagger}$ and enthalpy $\Delta H^{\ddagger}$ point to a dissociatively activated interchange, I_d, water exchange mechanism, as was typically observed for nine-coordinate complexes. So far, no water exchange data are known for structurally similar chelates. Among pyridine-derived chelates, the Gd^{3+} complex of a ligand with ethane-1,2-diamine backbone bearing pyridine units with carboxylate pendant arms has also been reported to have a water exchange rate similar to $[Gd(dota)(H_2O)]^-$.[17] On the other hand, the water exchange was 1–2 orders of magnitude faster on HOPO-type Gd^{3+} complexes, containing hydroxypyridinonate moieties, than on $[Gd(dtpa)(H_2O)]^{2-}$ or $[Gd(dota)(H_2O)]^-$. Particularly fast exchange was found for the dihydrated HOPO chelates.[18]

For dissociatively activated water exchange processes, the steric crowding around the water binding site is a very important factor to determine the rate of the exchange. A larger steric compression favors the departure of the coordinated water molecule in the rate-determining step, therefore contributes to a faster exchange.[19] The coordination of the bipyridine and the central amine nitrogen atoms, and the three carboxylate groups (overall CN = 8) does not seem to induce a strong steric compression around the water binding site to lead to a considerably faster water exchange than that on $[Gd(dtpa)(H_2O)]^{2-}$ or $[Gd(dota)(H_2O)]^-$.

Concerning the other parameters obtained in the simultaneous fit of the ^{17}O NMR and NMRD data, both the rotational correlation time and the electron spin relaxation parameters present common values corresponding to the size of the molecule.

Labeling of $Na[GdL(H_2O)]$ onto BSA and Relaxivity of the $[GdL(H_2O)]_n$–BSA Adduct

Slowing down the rotational mobility of a Gd complex is a well-known protocol to increase its relaxivity.[1] This can be achieved by weak interactions with large molecules,[20] supramolecular interactions,[21] or covalent linking on synthetic or naturally occurring macromolecules.[1b,22] The ability of the $[Ln\mathbf{L}(H_2O)]$ complexes to be covalently linked to macromolecules appeared as an efficient strategy to increase the rotational correlation time, and thus to obtain higher relaxivity. The Gd complex was therefore grafted on bovine serum albumin (BSA) according to the procedure used for europium and terbium complexes,[14] but replacing *N*-hydroxysuccinimide by its more water-soluble *N*-hydroxysulfosuccinimide analogue.[23] After purification by dialysis, a labeling ratio of 6.8 Gd complexes per BSA molecule was obtained by deconvolution of the UV/Vis absorption data of the labeled BSA. The Gd/BSA ratio is in excellent agreement with the previous experiments performed with the Eu and Tb analogues.

The values of longitudinal and transversal relaxivities of the Gd-labeled BSA at different fields are reported in Table 2 together with values obtained for the precursor $[Gd\mathbf{L}(H_2O)]^-$ complex.

Table 2. Values of longitudinal (r_1) and transversal (r_2) relaxivities for $[Gd\mathbf{L}(H_2O)]^-$ and $[Gd\mathbf{L}(H_2O)]_{6.8}$–BSA in water at varying fields (310 K).

Frequency [MHz] (Field [T])	$Gd\mathbf{L}[H_2O]^-$		$[Gd\mathbf{L}(H_2O)]_{6.8}$–BSA	
	r_1 [mM^{-1} s^{-1}]	r_2 [mM^{-1} s^{-1}]	r_1 [mM^{-1} s^{-1}]	r_2 [mM^{-1} s^{-1}]
20 (0.47)	3.5	3.7	7.3	8.6
40 (0.94)			7.4	9.8
60 (1.41)	3.3	3.8	7.5	10.4
300 (7.05)	3.5	4.4	5.1	12.5

The effect of the labeling on the relaxivities of the complex appeared to be rather modest with an increase of only a factor of 2, leading to values similar to those obtained for $[Gd(dtpa)(H_2O)]^{2-}$ grafted on a dextran polymer.[24] The luminescence data obtained on the isostructural Eu complex allows for a better understanding of the system. For Eu,[14] labeling on BSA resulted in an increase of the luminescence lifetime in water from 0.62 ms for $Na[Eu\mathbf{L}(H_2O)]$ to an average value of 1.10 ms for the labeled complex. This can be attributed to a substantial replacement of the coordinated water molecules in the protein-linked chelate by coordinating entities from the protein such as carbonylamides. According to the theoretical treatment developed by Horrocks and co-workers on the relationship between the number of coordinated water molecules and the luminescence lifetime of europium complexes,[7a–7c] the relative loss of coordinated water molecules can be estimated according

to Equation (1), in which τ_{EuLBSA} and τ_{EuL} stand for the europium luminescence lifetimes in the BSA adduct and in the unlabeled form, respectively.

$$\Delta q = 1.05 \times (1/\tau_{EuLBSA} - 1/\tau_{EuL}) \quad (1)$$

It can then be deduced that 70% of the europium complexes in the BSA-labeled adduct have lost their coordinated water molecule. The same scenario can be envisaged for the Gd complex, which is here translated into a decreased access of water and hence into a decreased relaxivity.

Synthesis and Photophysical Properties of the Dy and Sm Complexes

The dysprosium and samarium complexes of **L** were synthesized by mixing equimolar amounts of the ligand and lanthanide salts in water. For both complexes, elemental analysis and mass spectrometry data are in agreement with a formulation containing one ligand molecule per metal atom. Their IR spectra are in agreement with the presence of coordinated (1620 and 1645 cm^{-1} for Dy and Sm, respectively) and free (1590 cm^{-1} for both) carboxylate functions.

The main photophysical properties of the novel Dy and Sm complexes are gathered in Table 3, whereas Figure 2 represents their normalized emission spectra upon UV excitation (308 nm).

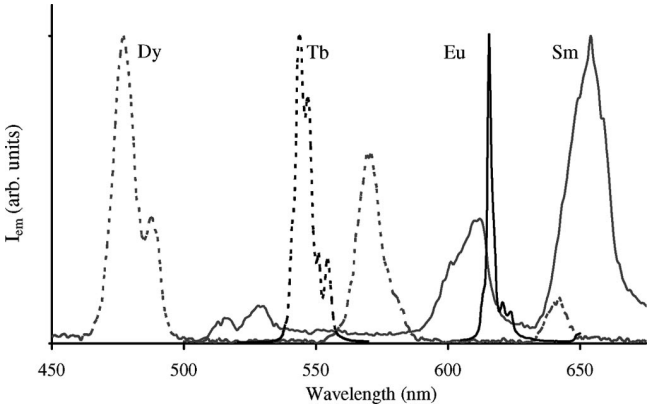

Figure 2. Emission spectra of Na[Dy**L**(H_2O)] (dashed gray) and Na[Sm**L**(H_2O)] (gray) in water [the main emission band of the Tb (dashed black) and Eu complexes (black) are also added for comparison]. For all compounds, spectra are normalized to their most intense emission band.

The UV/Vis absorption spectra of the complexes are composed of a main absorption band with a maximum at 308 nm, which corresponds to $\pi \rightarrow \pi^*$ transitions centered on the bipyridyl moieties.[25] Upon excitation into this absorption band, the emission spectra of the complexes displayed metal-centered emission characteristics of the f–f emission bands of the corresponding lanthanide complexes. For Dy, narrow emission bands were observed at 477, 571, and 642 nm (20960, 17500, and 15600 cm^{-1}, respectively) attributed to the $^4F_{9/2} \rightarrow {}^6H_{15/2}$, $^4F_{9/2} \rightarrow {}^6H_{13/2}$, and $^4F_{9/2} \rightarrow {}^6H_{11/2}$ transitions. Interestingly, a weak and large emission band centered around 440 nm (22700 cm^{-1}) was also evidenced in the emission spectrum of this complex. Regarding its energy, this band can be attributed to an emission from the $^3\pi\pi^*$ state, in excellent agreement with the energy level observed in the Gd complex at low temperature (22100 cm^{-1} at 77 K).[14] This behavior has already been observed for Dy complexes of cyclen derivatives[26] and was mainly explained by the selection rules on ΔJ which hinder an energy transfer from the ligand triplet state to the Dy $^4F_{9/2}$ state.[27] As often observed for Dy complexes,[13,25] the metal-centered emission quantum yield of the complex is rather low in water solution (Table 3). On the basis of the metal-centered luminescence excited-state lifetimes in water and D_2O, and using Equation (2), developed by Kimura and co-workers,[28] it was possible to estimate the hydration number of the complex, $q_{Dy} = 1.1 \pm 0.5$ water molecules in the first coordination sphere.

$$q_{Dy} = 2.11 \times 10^{-5}(k_{H_2O} - k_{D_2O}) - 0.60 \quad (2)$$

For Sm, the fluorescence spectra did not show the presence of the ligand-centered triplet emission. Narrow emission peaks were observed at 516 and 529 nm ($^4G_{5/2} \rightarrow {}^6H_{5/2}$), 612 nm ($^4G_{5/2} \rightarrow {}^6H_{7/2}$), and 654 nm ($^4G_{5/2} \rightarrow {}^6H_{9/2}$). The metal-centered luminescence quantum yield is also rather low in water, and the Sm-centered excited-state lifetimes in water and D_2O allowed the calculation of the hydration number according to Equation (3).[28]

$$q_{Sm} = 2.54 \times 10^{-5}(k_{H_2O} - k_{D_2O}) - 0.37 \quad (3)$$

A value of $q_{Sm} = 1.4 \pm 0.5$ water molecules was obtained pointing to one water molecule in the first coordination sphere (within experimental error) and to the isostructurality of the overall series of complexes from Sm to Dy. From the spectroscopic data (Table 3), it is worth noting that the series is well suited for covering emission in the visible region with a characteristic spectroscopic signature of each cation. Furthermore, the large difference in the luminescence lifetimes also offers the possibility of temporal discrimination of the emitted signals.

Luminescence Staining

As a proof-of-concept for use as a polyvalent reporter, the Tb complex was employed as a luminescent stain in time-resolved luminescence microscopy. Recently, lumines-

Table 3. Main photophysical properties of Na[Dy**L**(H_2O)] and Na[Sm**L**(H_2O)] in water and D_2O.

	Absorption	Metal luminescence properties		
	λ_{max} [nm] (ε_{max} [M^{-1} cm^{-1}])	$\tau^{300K}_{(H_2O)}$ [μs]	$\tau^{300K}_{(D_2O)}$ [μs]	$\phi^{300K}_{(H_2O)}$ [%]
Na[Dy**L**(H_2O)]	308 (21200)	6.8	15.5	0.7
Na[Sm**L**(H_2O)]	308 (21000)	11.4	60	0.2

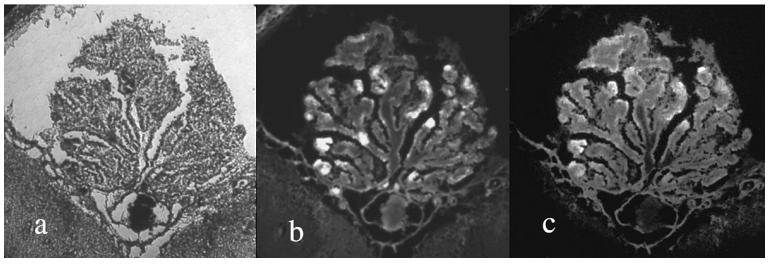

Figure 3. Transmission (a), prompt fluorescence (b), and time-resolved luminescence (delay time 100 μs) (c) microscopy images (real size 1 × 1 mm) of the region of the choroids plexus of rat brain slices stained with [Tb**L**(H_2O)]Na.

cent lanthanide complexes were shown to be good candidates for intracellular staining experiments in fluorescence mode.[29] Because of their high polarity, our complexes were postulated to be efficient reporters of local hydrophilicity. In order to support this hypothesis, rat brain slices[30] were stained by incubation in a water solution containing the Tb complex and were examined by time-resolved luminescence microscopy (TRLM).[31] The choice of rat brain was dictated by the simultaneous presence of regions of high hydrophobicity (parenchyma, gray matter) together with more hydrophilic regions such as blood vessels and the blood–brain barrier. Figure 3 displays images of the region of the choroid plexus in transmission mode, prompt fluorescence mode, and time-resolved luminescence mode (delay of 100 μs).

The region of the choroid plexus evidenced highly luminescent zones. The time-resolved acquisition mode allowed the elimination of the autofluorescence of the sample and light scattering in the microscope,[5] revealing the labeling with Tb to be particularly localized in the plexus domain, a part of the BBB mainly composed of hydrophilic epithelial cells. In contrast, regions of the gray matter surrounding this region are visible in prompt fluorescence, but these fluorescence signals disappeared upon imposition of a delay time between excitation and acquisition. The Tb complex was thus principally localized in hydrophilic regions of the brain and acted as a reporter of local hydrophilicity. This particularity should be of special interest regarding diseases such as encephalopathy in which the frontiers of the BBB are altered.[31]

Conclusions

Spectroscopic measurements on the Dy and Sm complexes of the bis(bipyridyl) ligand **L** combined with a ^{17}O and ^{1}H relaxation study on the Gd^{3+} analogue evidenced that all these complexes have a hydration number of one, pointing to an isostructural formulation for middle-lanthanide [Ln**L**(H_2O)]$^{-}$ complexes (from Sm to Dy). The photophysical properties of the luminescent Dy and Sm complexes are typical of those lanthanide ions and open perspectives for their use as luminescent probes in time-resolved acquisition mode. The relaxivity of the Gd complex is in line with that measured for typical (monoaqua)Gd complexes. The anchoring of the chelate on a large molecular framework such as BSA allowed for doubling of its relaxivity.

Lanthanide complexes of **L** represent a polyvalent family that can be used both as luminescent labels and MRI contrast agents. Their relevant photophysical and magnetic properties, combined with the possibility of easy covalent linkage to amino residues such as lysine could afford a wide range of applications. Staining experiments on rat brain slices evidenced the application in time-resolved luminescence microscopy, which can easily be targeted to more specific sites by immunochemistry.

Among possible applications, the similar complexation behavior of Tb and Gd offers the opportunity to use them as bimodal imaging probes, either in independent experiments or as mixtures of both labels. An interesting approach could be to use the Gd complex for macroscopic observations with concomitant microscopic analyses using the Tb label.

Experimental Section

Synthesis of the Complexes: Na[Ln**L**(H_2O)] complexes (Ln = Gd and Tb) were synthesized according to a literature procedure.[14]

Na[SmL(H_2O)]·3H_2O: LH_4·3HCl (40 mg, 59 μmol) was dissolved in a mixture of methanol (20 mL) and water (20 mL). To this solution was added a mixture of $Sm(OTf)_3$ (39 mg, 65 μmol) in methanol (3 mL) and water (3 mL). The solution was heated to 70 °C for 1 h. After the mixture was cooled to room temperature, the pH was brought to 7.0 with a 0.5% NaOH solution in water. The solution was concentrated under reduced pressure until a precipitate formed; thf was added to complete precipitation, and upon centrifugation, Na[Sm**L**(H_2O)]·3H_2O (35.6 mg, 76%) was isolated as a white powder. IR (KBr): $\tilde{\nu}$ = 3420, 1645, 1590, 1460, 1384 cm^{-1}. $C_{29}H_{21}N_5NaO_8Sm·4H_2O$ (812.96): calcd. C 42.75, H 3.56, N 8.60; found C 42.72, H 3.37, N 8.42. FAB^+/MS: *m*/*z* (%) = 743.1 (100) [NaSm**L** + H]$^+$, 721.2 (45) [Sm**L**H + H]$^+$.

Na[DyL(H_2O)]·4H_2O: LH_4·3HCl (40 mg, 59 μmol) was dissolved in a mixture of methanol (20 mL) and water (20 mL). To this solution was added a 40% solution of $Dy(ClO_4)_3$ in water (19 mg, 51 μmol) in methanol (3 mL) and water (3 mL). The solution was heated to 70 °C for 1 h. After the mixture was cooled to room temperature, the pH was brought to 7.0 with a 0.5% NaOH solution in water. The solution was concentrated under reduced pressure until a precipitate formed; thf was added to complete precipitation, and upon centrifugation, Na[Dy**L**(H_2O)]·4H_2O (32 mg, 67%) was

isolated as a white powder. IR (KBr): $\tilde{\nu}$ = 3420, 1620, 1590, 1464, 1387 cm^{-1}. $C_{29}H_{21}DyN_5NaO_8{\cdot}5H_2O$ (843.08): calcd. C 41.23, H 3.67, N 8.29; found C 41.54, H 2.47, N 8.29. FAB^{+-}/MS: *m*/*z* (%) = 755.1 (30) $[NaDyL + H]^+$, 733.2 (45) $[DyLH + H]^+$.

Labeling of BSA by [GdL(H_2O)]: Na[Gd**L**(H_2O)] (19 mg, 24 μmol) was suspended in dmso (5 mL), and the sodium salt of *N*-hydroxysuccinimido-3-sulfonic acid (7 mg, 30 μmol) and *N*-[3-(dimethylamino)propyl]-*N*′-ethylcarbodiimide hydrochloride (EDCI·HCl, 5 mg, 26 μmol) were added. The solution was agitated for 24 h. Addition of thf resulted in the formation of a pale yellow precipitate which was recovered by centrifugation and dried to afford [Gd**L**(H_2O)]* (19 mg, 80%). FAB^{+-}/MS: *m*/*z* (%) = 681.2 (100) $[M - C_5H_3NaNO_7S]^+$, 726.3 (40) $[M - C_4H_3NaNO_5S]^+$. IR (KBr): $\tilde{\nu}$ = 3442, 1713, 1635, 1414, 1384, 1229 ($\nu_{SO2asym}$), 1039 (ν_{SO2sym}) cm^{-1}. BSA (Acros, purity >96%) labeling was performed in borate buffer at pH = 7.0 using a 30-fold excess of activated Gd complex per BSA molecule. Labeled BSA was purified by dialysis with a 8000 Daltons cut-off filter at 4 °C for 24 h. The labeling ratio was determined by deconvolution of the optical density measured at 308 nm.

Proton Relaxivity Measurements: Proton nuclear magnetic relaxation dispersion (NMRD) profiles were recorded with a field cycling relaxometer (Field Cycling Systems, Oradell, New Jersey, USA) working between 0.24 mT and 1.2 T on 0.6 mL solutions contained in 10-mm o.d. tubes. Proton relaxation rates were also measured at 0.235 T, 0.47 T, 0.94 T, 1.5 T on Minispec PC-110, PC-120, PC-140, and mq-60 (Bruker, Karlsruhe, Germany). The additional relaxation rates at 7.05 T were obtained with a Bruker AMX-300 spectrometer (Bruker, Karlsruhe, Germany). Values at 4.7 T and 20 °C were measured with an SMIS spectro-imaging system.

^{17}O NMR Spectroscopy: The transverse ^{17}O relaxation rates ($1/T_2$) were measured on a Gd**L**(H_2O)$^-$ aqueous solution (1 mM; pH = 6.0) by the Carr–Purcell–Meiboom–Gill spin-echo technique in the temperature range 283–334 K, with a Bruker Avance 500 (11.75 T, 67.8 MHz) spectrometer. The temperature was calculated according to previous calibration with ethylene glycol and methanol.[32] Acidified water ($HClO_4$, pH = 3.8) was used as the external reference. Analysis of the ^{17}O NMR and ^1H NMRD experimental data was performed with Micromath Scientist version 2.0 (Salt Lake City, UT, USA). The reported errors correspond to one standard deviation obtained by the statistical analysis.

Absorption and Emission Spectroscopy: UV/Vis absorption spectra were recorded with a Uvikon 933 spectrometer. Emission and excitation spectra were recorded with a Perkin–Elmer LS50B (working in the phosphorescence mode) or a PTI Quantamaster spectrometer. When necessary (emission in the red) a Hamamatsu R928 photomultiplier was used. Luminescence decays were obtained with the PTI Quantamaster instrument over temporal windows covering at least five decay times with correction for light scattering. Luminescence quantum yields were measured according to conventional procedures,[33] with diluted solutions (optical density < 0.05), using [Tb**L**(H_2O)]Na in nondegassed water (Φ = 31%)[14] as the reference. Estimated errors are ±15%.

Rat Brain Slice Staining and Time-Resolved Luminescence Microscopy: In an immuno-histoluminescence test experiment, rat brain slices were incubated in a water solution of Na[Tb**L**(H_2O)], and the slices were examined by time-resolved luminescence microscopy with a DMLB fluorescence microscope equipped for time-resolved acquisition.[5b] Rats were killed[30] under pentobarbital deep anesthesia by perfusion through the left ventricle of 4% paraformaldehyde (PFA) freshly prepared in 0.1 M phosphate buffer PBS. Further fixation was made by maintaining the brains overnight in the same fixative. The tissues were next embedded in paraffin wax and sagittal sections (5 μm thick) were made using the microtome (Leica Instruments, Germany). Sections were first deparaffinated in toluene followed by rehydration in ethanol and washed three times in distilled water. Tissue sections were incubated 60 min with Na[Tb**L**(H_2O)] (0.5 mg mL^{-1}) at room temperature. The tissue sections were then washed three times with water.

Supporting Information (see footnote on the first page of this article): Full mathematical description of the fitting procedure for relaxivity measurements.

Acknowledgments

The authors thank Robert Muller, Luce van der Elst, and Corinne Pierart from the Department of Organic Chemistry – NMR Laboratory (University of Mons-Hainaut, Belgium) for performing NMRD studies. The French Ministère de le Recherche et des Technologies is gratefully acknowledged for financial support (ACI jeunes chercheurs no. 4116).

[1] a) A. E. Merbach, E. Toth in *The Chemistry of Contrast Agents in Medical Magnetic Resonance Imaging*, Wiley, London, **2001**; b) P. Caravan, J. E. Ellison, T. J. Mc Murry, R. B. Lauffer, *Chem. Rev.* **1999**, *99*, 2293–2352; c) M. Botta, *Eur. J. Inorg. Chem.* **2000**, 399–407.

[2] a) J. Wöhnert, K. J. Franz, M. Nitz, B. Imperiali, H. Schwalbe, *J. Am. Chem. Soc.* **2003**, *125*, 13338–13339; b) M. Prudencio, J. Rohovec, J. A. Peters, E. Tocheva, M. J. Boulanger, M. E. P. Murphy, H.-J. Hupkes, W. Kosters, A. Impagliazzo, M. Ubbink, *Chem. Eur. J.* **2004**, *10*, 3252–3260; c) R. S. Prosser, H. Bryant, R. G. Bryant, R. R. Vold, *J. Magn. Reson.* **1999**, *141*, 256–260.

[3] a) I. Hemmilä, R. Harju in *Biological Applications of Labelling Technologies* (Eds.: I. Hemmilä, T. Ståhlberg, P. Mottram), Wallac Oy and EG&G Cie Pb, Turku, Finland, **1995**, pp. 83–143; b) L. J. Charbonnière, N. Hildebrandt, R. Ziessel, H.-G. Löhmannsröben, *J. Am. Chem. Soc.* **2006**, *128*, 12800–12809.

[4] J. Chen, P. R. Selvin, *J. Am. Chem. Soc.* **2000**, *122*, 657–660.

[5] a) A. Beeby, S. W. Botchway, I. M. Clarkson, S. Faulkner, A. W. Parker, D. Parker, J. A. G. Williams, *J. Photochem. Photobiol. B* **2000**, *57*, 83–89; b) L. J. Charbonnière, N. Weibel, C. Estournes, C. Leuvrey, R. Ziessel, *New J. Chem.* **2004**, *28*, 777–781.

[6] R. D. Shannon, *Acta Crystallogr., Sect. A* **1976**, *32*, 751–767.

[7] a) W. W. De Horrocks Jr, D. R. Sudnick, *Acc. Chem. Res.* **1981**, *14*, 384–392; b) R. M. Supkowski, W. W. De Horrocks Jr, *Inorg. Chim. Acta* **2002**, *340*, 44–48; c) W. W. De Horrocks Jr, D. R. Sudnick, *J. Am. Chem. Soc.* **1979**, *101*, 334–340; d) A. Beeby, I. M. Clarkson, R. S. Dickins, S. Faulkner, D. Parker, S. Royle, A. S. de Sousa, J. A. G. Williams, M. Woods, *J. Chem. Soc. Perkin Trans. 2* **1999**, 493–503.

[8] L. J. Charbonnière, R. Ziessel, *Helv. Chim. Acta* **2003**, *86*, 3402–3410.

[9] a) S. I. Weissmann, *J. Chem. Phys.* **1942**, *10*, 214–217; b) N. Sabbatini, M. Guardigli, J.-M. Lehn, *Coord. Chem. Rev.* **1993**, *123*, 201–228.

[10] A. Congreve, D. Parker, E. Gianolio, M. Botta, *Dalton Trans.* **2004**, 1441–1445.

[11] S. Aime, E. Gianolio, D. Corpillo, C. Cavallotti, G. Palmisano, M. Sisti, G. B. Giovenzana, R. Pagliarin, *Helv. Chim. Acta* **2003**, *86*, 615–632.

[12] D. J. Bornhop, D. S. Hubbard, M. P. Houlne, C. Adair, G. E. Kiefer, B. C. Pence, D. L. Morgan, *Anal. Chem.* **1999**, *71*, 2607–2615.

[13] I. Nasso, C. Galaup, F. Havas, P. Tisnès, C. Picard, S. Laurent, L. Vander Elst, R. N. Muller, *Inorg. Chem.* **2005**, *44*, 8293–8305.
[14] N. Weibel, L. J. Charbonnière, M. Guardigli, A. Roda, R. Ziessel, *J. Am. Chem. Soc.* **2004**, *126*, 4888–4896.
[15] É. Tóth, L. Helm, A. E. Merbach, "Relaxivity of MRI Contrast Agents" in *Topics in Current Chemistry* (Ed.: W. Krause), Springer-Verlag, Berlin, **2002**, vol. 221, chapter 2, pp. 61–101.
[16] D. H. Powell, O. M. Ni Dbubhghaill, D. Pubanz, L. Helm, Y. S. Lebedev, W. Schlaepfer, A. E. Merbach, *J. Am. Chem. Soc.* **1996**, *118*, 9333–9346.
[17] C. Platas-Iglesias, M. Mato-Iglesias, K. Djanashvili, R. N. Muller, L. Vander Elst, J. Peters, A. de Blas, T. Rodríguez-Blas, *Chem. Eur. J.* **2004**, *10*, 3579–3590.
[18] D. M. J. Doble, M. Botta, J. Wang, S. Aime, A. Barge, K. N. Raymond, *J. Am. Chem. Soc.* **2001**, *123*, 10758–10759.
[19] S. Laus, R. Ruloff, É. Tóth, A. E. Merbach, *Chem. Eur. J.* **2003**, *9*, 3555–3566.
[20] P. Caravan, N. J. Cloutier, M. T. Greenfield, S. A. McDermid, S. U. Dunham, J. W. Bulte, J. C. Amedio Jr, R. J. Looby, R. M. Supkowski, W. D. Horrocks Jr, T. J. Mc Murry, R. B. Lauffer, *J. Am. Chem. Soc.* **2002**, *124*, 3152–3162.
[21] J. B. Livramento, E. Toth, A. Sour, A. Borel, A. E. Merbach, R. Ruloff, *Angew. Chem. Int. Ed.* **2005**, *44*, 1480–1484.
[22] A. Datta, J. M. Hooker, M. Botta, M. B. Francis, S. Aime, K. N. Raymond, *J. Am. Chem. Soc.* **2008**, *130*, 2546–2552.
[23] N. Hildebrandt, L. J. Charbonnière, M. Beck, R. F. Ziessel, H.-G. Löhmannsröben, *Angew. Chem. Int. Ed.* **2005**, *44*, 7612–7615.
[24] N. Siauve, O. Clement, C.-A. Cuenod, S. Benderbous, G. Frija, *Magn. Reson. Imaging* **1996**, *14*, 381–390.
[25] S. Comby, D. Imbert, A.-S. Chauvin, J.-C. G. Bünzli, L. J. Charbonnière, R. F. Ziessel, *Inorg. Chem.* **2004**, *43*, 7369–7379.
[26] G. Zucchi, A.-C. Ferrand, R. Scopelliti, J.-C. G. Bünzli, *Inorg. Chem.* **2002**, *41*, 2459–2465.
[27] G. F. De Sá, O. L. Malta, C. D. Donega, A. M. Simas, R. L. Longo, P. A. Santa-Cruz, E. F. da Silva, *Coord. Chem. Rev.* **2000**, *196*, 165–195.
[28] T. Kimura, Y. Kato, *J. Alloys Compd.* **1998**, *275*, 806–810.
[29] a) J. Yu, D. Parker, R. Pal, R. A. Poole, M. J. Cann, *J. Am. Chem. Soc.* **2006**, *128*, 2294–2299; b) R. A. Poole, G. Bobba, M. J. Cann, J.-C. Frias, D. Parker, R. D. Peacock, *Org. Biomol. Chem.* **2005**, *3*, 1013–1024; c) A. S. Chauvin, S. Comby, B. Song, C. D. B. Vandevyver, F. Thomas, J.-C. G. Bünzli, *Chem. Eur. J.* **2007**, *13*, 9515–9526.
[30] Please note, rats were not killed only for the purpose of this experiment, but were used previously as blanks in a clinical study.
[31] I. J. Namer, J. Steibel, P. Poulet, J. P. Armspach, M. Mohr, Y. Mauss, J. Chambron, *Brain* **1993**, *116*, 147–159.
[32] D. S. Raiford, C. L. Fisk, E. D. Becker, *Anal. Chem.* **1979**, *51*, 2050–2051.
[33] Y. Haas, G. Stein, *J. Phys. Chem.* **1971**, *75*, 3668–3677.

Received: March 13, 2008
Published Online: May 15, 2008

